2014 IEEE International Conference on Robotics & Automation (ICRA)
Hong Kong Convention and Exhibition Center
May 31 - June 7, 2014. Hong Kong, China

Insect-inspired Thoracic Mechanism with Non-linear Stiffness for Flapping-Wing Micro Air Vehicles

Yao-Wei Chin, Joel Tian-Wei Goh, Gih-Keong Lau
School of Mechanical and Aerospace Engineering, Nanyang Technological University, Singapore 639798

Abstract— **This paper presents the design, analysis and characterization of a compliant mechanism that saves power for flapping-wing micro-air vehicles (FWMAV). The compliant mechanism is shaped after the insect's flight thorax, which has integrated elastic hinges for energy storage. It shows a nonlinearly increasing stiffness, which slows the wings down rapidly toward the end of a wing stroke and reverses the wings quickly, just like the elastic radial stop in Dipteran insects. When used to drive a 10-cm wing span FWMAV, it saves power up to 31% in comparison to a conventional rigid-body flapping mechanism, which have no elastic storage capability.**

I. INTRODUCTION

Flapping-wing flight is agile but could be energetically cost to hover. [1] [2] Substantial power is expended to move air and wings [3] [4]. Aerodynamic power is incurred to produce lift and overcome drag in air. In addition, inertial power is needed to accelerate the wing from rest at the beginning of a stroke and then decelerate it to a rest at the end of the stroke [1] [4]. This inertial power increases greatly with frequency and can take up as much as 53% of the total flight power during hovering. [5] In comparison, less agile rotary wing flight by helicopter is energetically more efficient during hovering because it does not need to accelerate and decelerate the rotary wing blades [6].

However, entomologists and aerodynamicists found that insects had a way to reduce the inertial power by elastic energy storage in their flight apparatus [2] [7] [8]. Insect has elastic elements in their flight muscles [9], flight thorax, and wing hinges [2] [3]. In *Dipteran* insects, each wing rotates about a fulcrum at the pleural process of their flight thorax when their muscles contract to deform the thorax. At the end of wing stroke, wing momentum is converted into elastic energy, in the deformed elastic elements. The elastic energy is recovered during wing reversal in assistance to flight muscles [3] [10]. Hence, most power output by the insect flight muscles is expended on aerodynamic power, and little is needed for inertial power.

In contrast, most flapping wing micro air vehicles (FWMAV) are not capable of storing elastic energy (DelFly [6], Nano-Hummingbird [11]). An electric motor itself that powered the MAV cannot store elastic energy. Rigid body mechanisms for common FWMAV have no elastic element to recover the inertial power. Hence, most FWMAVs are limited to short flight endurance because wing reciprocation requires high inertial power in addition to aerodynamic power.

Recently, some researchers have attempted elastic energy storage by including discrete springs in the motor-powered rigid-body mechanism for flapping wings. Madangopal et al [12] showed by simulation that inclusion of linear coil springs, which connect wing roots to the ground of a crank-rocker mechanism, can reduce the peak torque required from a motor as much as 12%, whereas Tantanawat and Kota [13] showed by simulation that it could reduce the peak input power as much as 42%. Baek and Fearing [14] showed by experiment that incorporation of a linear coil spring in a crank slider mechanism can save motor power as much as 19% in the presence of friction in the revolute-joined mechanism. However, discrete springs increase payload of the FWMAV and do not help to reduce friction in the mechanism.

However, compliant mechanism could be used to store elastic energy inherently and be free of friction. A thorax-like compliant mechanism could be man-made using lightweight composites. Recently, Wood has developed 3cm span Robotfly using carbon fibre reinforced polymer (CFRP) as the exoskeleton plates and polyimide film as the flexible hinges to build compliant thoracic mechanism, with elastic energy storage in the piezoelectric actuator [15]. However, it is not clear if the compliant thoracic mechanism could store enough elastic energy for a larger scale motorized FWMAV (10-15cm wing span, 3g and more) [16]. In Sahai's attempt [17], thick elastomeric strips are used to store the required elastic energy instead of the polyimide hinges. Stiffer polyimide hinges can store more elastic energy, but they are susceptible to fatigue fracture due to high cyclic loading by large wing stroke.

In this paper, we present a lightweight compliant thoracic mechanism with multiple-stiffness polyimide hinges that could store elastic energy required for FWMAV with a 100mm wing span, larger than most insects'. The thoracic mechanism is a close-form shell consisting of rigid plates connected by flexible hinges. The hinges are made of different stiffness to have large wing stroke and high energy storage. Like insects, it produces wing flapping motion when its tergal plate is reciprocated. The tergal depression manifested a nonlinearly increasing stiffness, which slows the wings down rapidly at the end of a wing stroke and reverses the wings quickly, just like the elastic radial stop in Dipteran insects [18]. We further show that power saving is effective only if elastic energy storage is sufficient to recover the inertial power, below the resonant frequency of the thoracic mechanism.

978-1-4799-3684-7/14/$31.00 ©2014 IEEE

II. Thoracic Mechanism

A. Insect-inspired Design

Insects' flight thorax, which on which the wings attached, has a sophisticated anatomy. However, it could be visualized as a ring of exoskeleton plates and hinges. The exoskeleton plates are made of tough *chitin*, while the wing hinges are composed of softer elastic *resilin*. The ring has the side (pleura) and the base (sternum) walls fused together, while the wings hinged on the pleura and the wing base is joined to the tergum. [19] When its tergum plate is depressed by flight muscles, the thorax flaps the wings upwards. Upon muscles relaxation, the thorax restores to its unloaded shape and releases the stored elastic energy in assistance to muscles for reversing the wing stroke.

Such thorax could be made using lightweight composite compliant mechanism. Like Wood's Robotfly thorax, we use CFRP as rigid plates and polyimide films as hinges. However, the compliant thoracic mechanism is designed as a closed-form composite shell with a non-linear stiffness characteristic, which store up elastic energy at increasing rate when deformed further. Its symmetry half appears like four-bar linkages with elastic polyimide hinges (Fig. 1). It is activated by a motor through a crank-slider mechanism that reciprocates a tergal plate of the thorax. Like the insect thorax, tergum depression bends the polyimide hinges of the wing base and produces an upward wing stroke (Fig. 2).

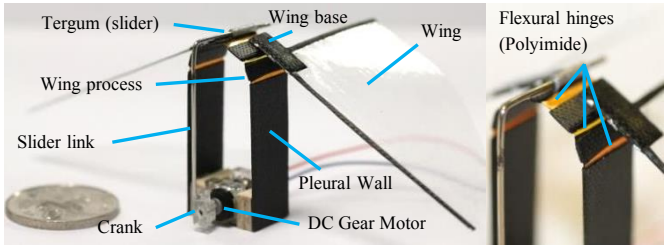

Fig. 1 Compliant thoracic mechanism with integrated elastic energy storage in the polyimide hinges.

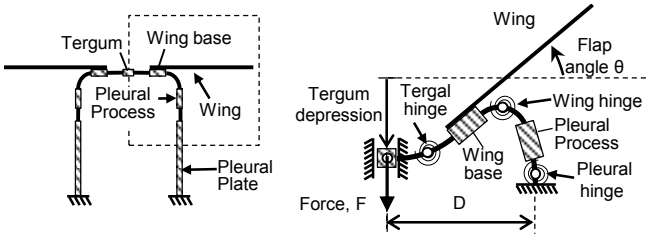

Fig. 2 Activation of the compliant mechanism under a force at the tergum

To meet the needs for a large wing stroke and enough elastic energy storage without risking fracture, multiple-stiffness flexural hinges are used in the thoracic mechanism. There are three elastic hinges in a half thorax. The wing hinge is designed to have the least stiffness to allow large wing stroke. The tergal hinge is made slightly stiffer to transfer the actuation force from tergum to the wing base but also bend for the wing rotation. The pleural hinge is stiffest because it bends only a little and so act as the main energy storage. This compliant mechanism exhibits a low stiffness when the wing is at the neutral stroke and moves at the highest speed. However, it shows an increasingly high stiffness at the end stroke, where the wing stops and reverses. To minimize undesired twisting of hinges, the hinge length is designed to be small compared to width.

B. Analysis

The amount of elastic energy storage is important for the thorax design. Yet, it changes nonlinearly with the hinge deformation and large rotations of the linkages. To simplify the analysis, a symmetric half of the thorax is modeled as a pseudo-rigid model, which consists of rigid linkages and joints with torsional spring (Fig. 3). In this pseudo model, the tergum plate is represented by the slider on the symmetric half. Meanwhile, wing base and pleural process are represented by two linkages of length D and L respectively. The polyimide hinge between the rigid plates is represented by a revolute joint and a torsional spring. The equivalent linkage length is the sum of the plate length and half of the hinge lengths, at its two ends. The pleural process linkage is connected to the pleural wall (ground) through a spring with rotational stiffness K_0, and the wing base through a spring with rotational stiffness K_1. The wing base linkage connects to the pleural process through a spring with rotational stiffness K_1 and tergum through a spring with rotational K_2.

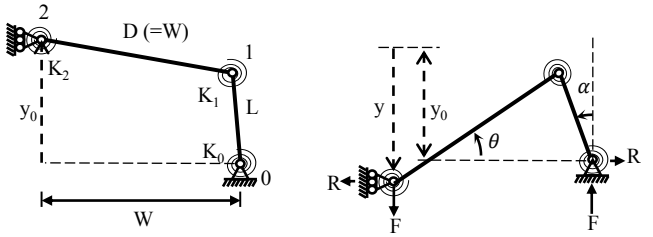

Fig. 3 Pseudo-rigid model of the half thorax with the wing base in static equilibrium of its neutral state and activated state.

When not loaded, the tergum is statically positioned at the neutral point h. The unloaded wing attitude is angled slightly downward. To create an upward wing stroke, the tergum is depressed by a force F and travels a displacement y from the initial height y_0. As a result of tergum depression, the wing lever of length D rotates by an angle θ (relative to the horizontal) whiles the pleural process of length L rotates by and angle α (relative to the vertical). The tergum height off the pleural-process hinge is related to the plate rotations, following:

$$y = y_0 + D \sin\theta - L \cos\alpha \quad (1)$$

To achieve a static wing stroke of 60°, typical to FWMAV, a crank length of 3mm is chosen to reciprocate the tergum with a total displacement of 6mm, up to down about the neutral point. Distance between the anchors of pleural wall to the symmetry plane, over which the two linkages span, remains a constant W. This yields the following constraint equation:

$$W = D \cos\theta + L \sin\alpha \quad (2)$$

Depressive force on the tergum is resisted by the deformed torsional springs in the thoracic compliant mechanism. It can be determined from force analysis of individual linkages. Moment equilibrium for the pleural process linkage of length L yields:

$$K_0\alpha + K_1\left(\theta - \alpha + \frac{\pi}{2}\right) - FL\sin\alpha + RL\cos\alpha = 0 \quad (3)$$

Moment equilibrium for wing base linkage of length D yields:

$$K_1\left(\theta - \alpha + \frac{\pi}{2}\right) + K_2(\theta) - FD\cos\theta - RD\sin\theta = 0 \quad (4)$$

Flexural hinge stiffness K_0, K_1, and K_2 are given as [20]:

$$K = \frac{dM}{d\theta} = \frac{EI}{H} \quad (5)$$

where E is the Young's Modulus, $I = bt^3/12$ is the area moment of inertia about the bending axis, and H, b and t being the length, width and thickness of the hinge respectively.

Solving the tergum force (half thorax only) as in terms of angles yields:

$$F = \frac{\left\{K_0\alpha + \left[K_1\left(\theta - \alpha + \frac{\pi}{2}\right)\right]\left(1 + \frac{L\cos\alpha}{D\sin\theta}\right) + K_2(\theta)\frac{L\cos\alpha}{D\sin\theta}\right\}}{L\left(\sin\alpha + \frac{\cos\alpha\cos\theta}{\sin\theta}\right)} \quad (6)$$

Table 1 summarizes current design parameters chosen to produce a static wing stroke of 60°given ±3mm of tergum reciprocation by a 6-mm diameter coreless DC motor. The stiffness is chosen to store elastic energy that matches the maximum wing kinetic energy at 30Hz, assuming same wing stroke. The design is not dynamically optimized because the dynamic response in terms of wing stroke is unknown.

Table 1 Parametric values for the pseudo rigid model

Parameter	Input Value
D=W	6 mm
L	3.692 mm
K_0	4.267 mNm/rad
K_1	0.03414 mNm/rad
K_2	0.1366 mNm/rad

When deformed, this thoracic mechanism produces a wing stroke, which increases in linear proportion to the tergum depression. Fig. 4 show the wing sweeps 10° per 1 mm tergum depression. However, the force required to depress the tergum increases non-linearly with the tergum displacement as in Fig. 5. The theoretical prediction agrees well in trend with the experimental measurements.

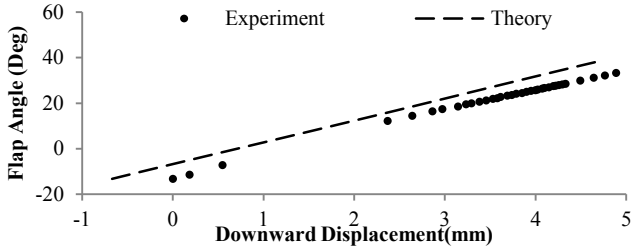

Fig. 4 Static wing flap angle increment with tergum downward displacement for the compliant mechanism

The elastic energy stored in the deformed thoracic mechanism is equal to the work done by the depressive force F on the tergum. Integration of the force over the tergum displacement y, which starts from the neutral position to the down most position y_{max}, yields:

$$W_{elastic} = \int_0^{y_{max}} F dy \quad (7)$$

Experiment showed that this thoracic mechanism can stored up to 0.4937mJ (50.3 g-f.mm) when the tergum is displaced down by 4.20 mm to produce a 33.2° wing flap. In comparison, theoretical model overestimate the value to be 2.492mJ (240g-f.mm) at 4.31mm tergum displacement.

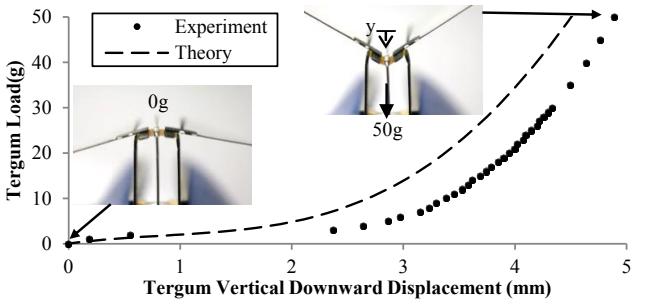

Fig. 5 Static force required to induce downward displacement of tergum (entire thorax) for compliant mechanism

C. Fabrication

The compliant thorax is made of CFRP plates (HexPly M10R/38%/UD150/CHS) and polyimide film hinges (DuPont Kapton HN). The thoracic shell is an assembly and fold-up of three pieces of integrated hinge on plates. Each piece of the integrated hinge on plates is prepared by reinforcing a blank strip of polyimide film with CFRP patches. Its fabrication is done by using vacuum bagging method that lays up and cures CFRP prepregs on a flat polyimide film. The reinforced patches form the CFRP plates with the cured thickness of 3.2mm, while the unreinforced spacing of the polyimide film forms the hinge. Assembly between the pieces is done by adhesive bonding.

The flexural hinges are fabricated with different thickness and length to achieve the designed stiffness. The tergal hinge is of 0.0508 mm thick (2mil). The wing hinge that connects wing base to the wing process is a soft 0.0254mm (1mil) thin polyimide film while the pleural hinge is stiffest using 0.127mm (5mil) thick polyimide film.

The wing is made of 25μm thick polyester film of quarter-elliptical shape, with the leading edge length of 5cm and root chord of 3.1cm, at the aspect ratio of 4. The leading edge is reinforced with CFRP on both sides such that it is rigid span wise. The root chord is softer with single-side CFRP reinforcement to allow passive rotation about the leading edge.

D. Benchmark Rigid Body Mechanism

To illustrate the benefit of elastic storage, a compliant mechanism needs to be compared with a rigid-body counterpart. Unlike the rigid-body mechanism with discrete springs, a compliant mechanism does not have an identical rigid-body counterpart. Replacing elastic hinges from the compliant mechanism will yield an under-constraint mechanism that does not work. For comparison, the rigid-body counterpart is chosen to be a pair of rigid wing levers (Fig. 6), pivoted at a fulcrum each, such that the wing base has the same length D as its compliant mechanism counterpart (Table 2).

This rigid body benchmark (Fig. 7) is equipped with the same wing and it beats an 80° wing stroke using a 5mm crank. With similar wing stroke and kinematics at 20-30Hz, the rigid-body counterpart is expected to produce the same aerodynamic and inertial work as the compliant mechanism. At the same basis of aerodynamic and inertial work output, energy input saving could be attributed to the effect of elastic energy storage in the mechanism.

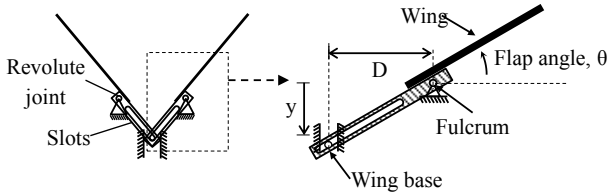

Fig. 6 A rigid body wing flapper with the wing levered on a revolute joint and flapped up by θ when its base is moved down by y.

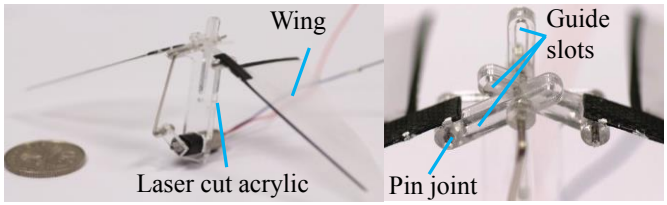

Fig. 7 The rigid body mechanism prototype without any energy storage for comparison

Table 2 Comparison of the compliant mechanism and the rigid body mechanism design

Parameters	Compliant Mechanism	Rigid Body Mechanism
Dynamic wing stroke	77° @ >20Hz	85° @>0Hz
Wing span	100mm	100mm
Wing Moment of Inertia	7.205×10^{-8}kgm^2	7.205×10^{-8}kgm^2
Lever Arm	7mm	7mm
Crank length	3mm	5mm
Weight	3.51g	3.34g

III. Energetic Costs Analysis

A. Power Requirements of Flapping Flight

Flapping flight of micro air vehicle demands a lot of power. Firstly, aerodynamic power is expended in moving the wings against air. Secondly, inertial power is also required to accelerate and decelerate the wings. Thirdly, if there is embedded spring for elastic energy storage, elastic power is required to compress the spring though recovered upon the spring back. Lastly, friction in transmissions and motor causes dissipative loss. To sum up, the total mechanical power (P_{mech}), i.e. the cost incurred by flapping flight, is a sum of the aerodynamic power (P_{aero}), inertial power ($P_{inertial}$), elastic power ($P_{elastic}$), and friction losses (P_{losses}):

$$P_{mech} = P_{aero} + (P_{inertia} + P_{elastic}) + P_{losses} \quad (8)$$

Ideally, the inertial power could convert fully into elastic power and vice versa like an oscillating spring-mass system, thus conserving energy within the system. The apparent power drawn from motor for these two components is zero if they are same in magnitude with no loss:

$$P_{inertial} + P_{elastic} = 0 \quad (9)$$

The inertial power depends on the wing kinematics. Average inertial power of a sinusoidal wing stroke can be estimated from the maximum change of wing kinetic energy over a quarter cycle of the wing beat, where the speed peaks at the mid-stroke [4] [5]:

$$\bar{P}_{inertial} = 4\pi^2\phi^2 f^3 J_0 \quad (10)$$

where f is the wing beat frequency, ϕ is the wing stroke angle, and J_0 is the rotational inertia of each wing.

The average elastic power is the energy stored or released from the elastic thorax during a quarter cycle and worked against the inertial power:

$$\bar{P}_{elastic} = -4fW_{elastic} \quad (11)$$

B. Design of Experiment

Both the compliant mechanism and rigid-body mechanism are subjected to the same tethered flight tests. They are designed to beat the same wings with the same wing stroke, and consequently produce almost the same thrust at the same wing beat frequency. The two differed only in the capability for energy storage. As such, any power saving by the compliant mechanism should reflect the effect of the elastic energy storage. In the experiments, wing stroke angle is measured by imaging processing; quasi-steady thrust is measured using the pendulum swing method (see Fig. 8). The thrust provides the lift that raises the flapper up as frequency increases, like the thrust from helicopter rotor. The power consumed by the motor to drive a wing flapper can be measured using a source-measure unit, which can resolve time varying electrical signals. As such, mechanical torques and power can be deduced from the electrical measurement.

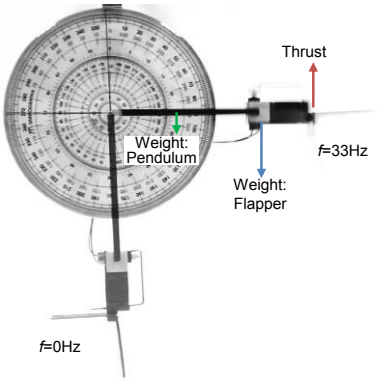

Fig. 8 Tethered hovering flight test using a simple pendulum method: The idle flapper is at bottommost position under the effect of gravity; when the wing flappers are beating at 33 Hz, thrust is produced to raise the pendulum of wing flappers above the horizon against gravity.

The prototypes are first driven with wings in air to obtain the total mechanical cost. Then, the aerodynamic power is removed by flapping in vacuum, to obtain apparent inertial power and friction loss. Lastly, prototypes are operated without wings to get friction loss. Hence, the power differences due to these distinct conditions should provide a measure for each component of energetic costs. All tests were carried out multiple times to minimize random error.

The dynamic coupling of the non-linear wing-thorax system is left for future investigation as energetic costs are of more concern in this study.

C. Results and Discussions

Both mechanisms beat wing in sinusoidal profile over time (Fig. 9). They have almost the same dynamic wing stroke at 22Hz and above (see Fig. 10), though compliant mechanism has a much lower static stroke. The enhancement of dynamic wing stroke over the static one is attributed to hinge flexibility of compliant mechanism.

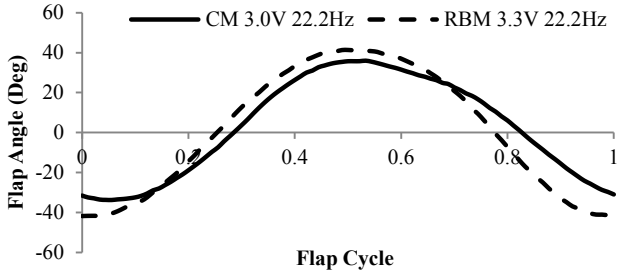

Fig. 9 Flapping trajectory observed using high speed camera.

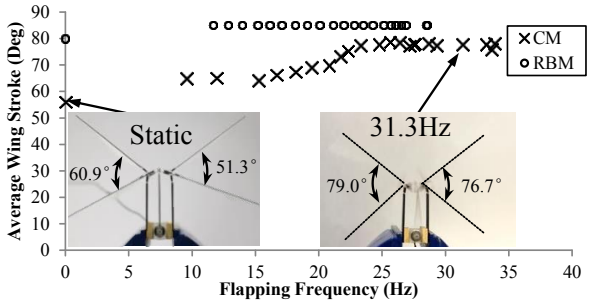

Fig. 10 Wing stroke observed along frequency for both compliant mechanism and rigid body mechanism.

As the wing beats faster, more thrust is generated (Fig. 11) at the expense of more power (Fig. 12). Both mechanisms produce almost the same thrust at the wing beat frequency of 22Hz and above. However, the compliant mechanism consumes less power. To lift up its own weight, the compliant mechanism consumes about 1.5W and presents a power savings of 22% as compared to the rigid body mechanism.

After all, the energetic costs to beat wings increase with wing beat frequency in both air and vacuum, so does the friction loss (see Fig. 13 and Fig. 14). Comparison of each power components showed that apparent inertial power is almost zero up to 25Hz, beyond which the wing kinetic energy exceeds the elastic energy storage capacity. In comparison, the rigid body mechanism expended substantially large portion of total power on overcoming wing inertia throughout the whole frequency range tested. At 30Hz, near take off, the compliant mechanism expends only 16% of total power to overcome inertia, while rigid body mechanism consumes higher power at 36% (see Fig. 15). In short, the elastic energy storage helped to reduce the inertial power for flapping flight.

Compared to other reported designs, our thorax-like compliant mechanism successfully integrated sufficient elastic energy storage within the lightweight compliant hinges (see Table 3). All other designs required elastic elements to be added to the mechanism.

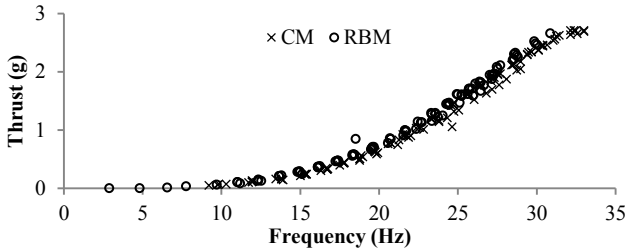

Fig. 11 Similar thrust measured along frequency for the prototypes.

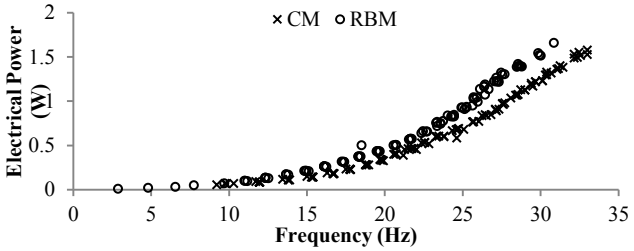

Fig. 12 Average electrical power input along frequency.

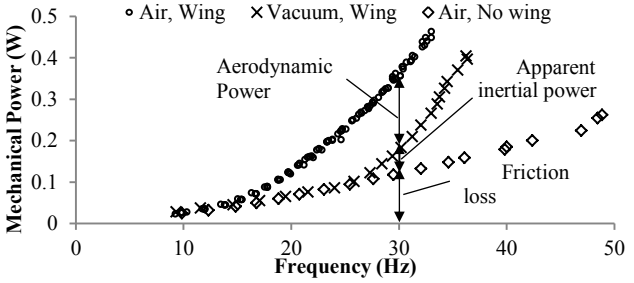

Fig. 13 Mechanical cost components for compliant mechanism. Apparent inertial power is almost zero at lower frequency range.

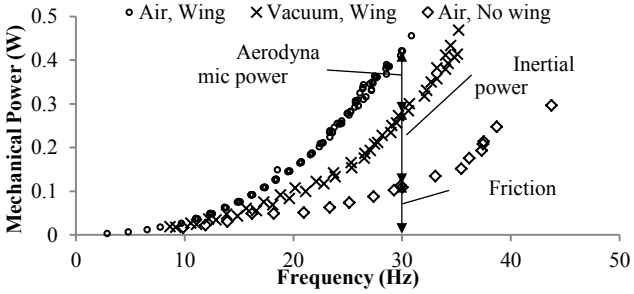

Fig. 14 Mechanical cost components for rigid body mechanism.

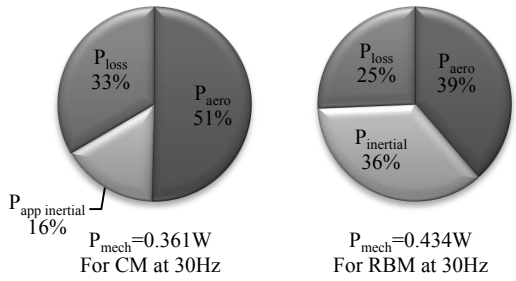

Fig. 15 Comparison of the mechanical power components between the compliant mechanism and rigid body mechanism.

Table 3 Comparison of the mechanism and elastic element in literature and our thorax-like compliant mechanism

Designs	MAV Weight	Wing Span (tip-to-tip)	Wing stroke	Flapping Frequency	Spring Type	Spring Stiffness	Spring/ Flexure Weight	Input Power Savings
Our CM	3.51g	100mm	56°-80°	9-33Hz	Closed Form Shell	0-700N/m	0.066g	31% max
Baek CM [14]	5.8g	80mm^	~55°	10-30 Hz	Linear Coil Spring	140N/m	0.259g*	30% max
Baek Vamp RC (RBM) [14]	13g	304.8mm (12 ")	45°	16Hz	Linear Coil Spring	980N/m	0.444g+	19% max
Sahai CM [17]	3g#	124mm	-	16-18Hz	Rubber Strips	3.2mN.m /rad	0.02g	20% max
Madangopal Simulation RBM [12]	-	600mm	90°	0.8Hz	Linear Coil Spring	51.3N/m	-	Peak torque 8-12%
Tantanawat Simulation RBM [13]	-	660mm	44.8°	4Hz	Linear Coil Spring	38N/m	-	Peak Input Power 42%

^ Estimated from photo image

* Estimated using wire diameter 0.44mm, coil diameter 5.5mm, spring free length of 21.5mm, 10 active coils, with Phosphorous Bronze Grad A (Young modulus 103GPa, density 8860kg/m3)

+ Estimated using wire diameter 0.65mm, coil diameter 5.5mm, spring free length of 21.5mm, 8 active coils, with Phosphorous Bronze Grad A.

Projected weight of the MAV design of which the mechanism is to be used.

Note: CM denotes compliant mechanism, RBM denotes rigid body mechanism

IV. Conclusion

We presented a thorax-like composite compliant mechanism with integrated elastic energy storage. Sufficient energy is stored in the multiple-stiffness hinges which are configured to achieve large wing stroke at low risk of fatigue fracture. Our results showed that elastic energy storage saves power by recovering wing inertial power. The power savings is optimum when the elastic energy storage matches the wing kinetic energy. However, the introduction of elastic energy storage should not add significant payload which cancels out power savings. Therefore, our method of integrating desired elastic energy storage into lightweight compliant mechanism can be used for future energy-efficient FWMAV.

References

[1] U. M. Norberg, T. H. Kunz, J. F. Steffensen, Y. Winter and O. V. Helversen, "The Cost of Hovering and Forward Flight in a Nectar-Feeding Bat, Glossophaga Soricina, Estimated from Aerodynamic Theory," *Journal of Experimental Biology,* vol. 182, pp. 207-227, 1993.

[2] T. Weis-Fogh, "Energetics of Hovering Flight in Hummingbirds and in Drosophila," *Journal of Experimental Biology,* vol. 56, pp. 79-104, 1972.

[3] R. F. Chapman, The Insects: Structure and Function, 4th ed., Cambridge: Cambridge University Press, 1998.

[4] C. P. Ellington, "The Aerodynamics of Hovering Insect Flight. VI Lift and Power Requirements," *Philosophical Transactions of the Royal Society of London. B,* vol. 305, no. 1122, pp. 145-181, 1984.

[5] C. v. D. Berg and J. M. V. Rayner, "The Moment of Inertia of Bird Wings and The Inertial Power Requirement for Flapping Flight," *Journal of Experimental Biology,* vol. 198, pp. 1655-1664, 1995.

[6] D. Lentink, S. Jongerius and N. Bradshaw, "The scalable design of flapping micro air vehicles inspired by insect flight," in *Flying insects and robots*, Springer-Verlag Berlin Heidelberg, 2009, pp. 185-205.

[7] C. Ellington, "Power and Efficiency of Insect Flight Muscle," *Journal of Experimental Biology,* vol. 115, pp. 293-304, 1985.

[8] T. Weis-Fogh, "Quick Estimates of Flight Fitness in Hovering Animals, Including Novel Mechanism for Lift Porduction," *Journal of Experimental Biology,* vol. 59, pp. 169-230, 1973.

[9] R. M. Alexander and H. C. Bennet-Clark, "Storage of elastic strain energy in muscle and other tissues," *Nature,* vol. 265, pp. 114-117, January 1977.

[10] M. H. Dickinson, "Muscle Efficiency and Elastic Storage in the Flight Motor of Drosophila," *Science,* vol. 268, no. 5207, pp. 87-90, 7 April 1995.

[11] M. Keennon, K. Klingebiel, H. Won and A. Andriukov, "Development of the Nano Hummingbird: A Tailless Flapping Wing Micro Air Vehicle," in *60th AIAA Aerospace Sciences Meeting Including the New Horizons Forum and Aerospace Exposition*, Nashville, Tennessee, 9-12 January 2012.

[12] R. Madangopal, Z. A. Khan and S. K. Agrawal, "Biologically Inspired Design Of Small Flapping Wing Air Vehicles Using Four-bar Mechanisms and Quasi-steady Aerodynamics," *Journal of Mechanical Design,* vol. 127, no. 4, pp. 809-816, 2005.

[13] T. Tantanawat and S. Kota, "Design of Compliant Mechanisms for Minimizing Input Power in Dynamic Applications," *Journal of Mechanical Design,* vol. 129, no. 10, pp. 1064-1075, 2007.

[14] S. S. Baek, K. Y. Ma and R. S. Fearing, "Efficient Resonant Drive of Flapping-Wing Robots," in *The 2009 IEEE/RSJ International Conference on Intelligent Robots and Systems*, St. Louis, USA, 2009.

[15] R. Wood, "Liftoff of a 60mg flapping-wing MAV," in *2007 IEEE/RSJ International Conference on Intelligent Robots and Systems*, San Diego, CA, USA, 2007.

[16] J. H. Marden, "Maximum Lift Production During Takeoff in Flying Animals," *Journal of Experimental Biology,* vol. 130, pp. 235-238, 1987.

[17] R. Sahai, K. C. Galloway and R. J. Wood, "Elastic Element Integration for Improved Flapping-Wing Micro Air Vehicle Performance," *IEEE Transactions on Robotics,* vol. 29, no. 1, pp. 32-41, 2013.

[18] A. R. Ennos, "A Comparative Study of The Flight Mechanism of Diptera," *Journal of Experimental Biology,* vol. 127, pp. 355-372, 1987.

[19] P. J. Gullan and P. S. Cranston, The Insects: An Outline of Entomology 4th Ed, Wiley-Blackwell, 2010.

[20] L. L. Howell, Compliant Mechanisms, New York: John Wiley & Sons, Inc, 2001.